PHYSICAL REVIEW D **96,** 014503 (2017)

Confinement-deconfinement transition in an $SU(2)$ Higgs theory

Minati Biswal,[1,*] Mridupawan Deka,[1,2,†] Sanatan Digal,[1,‡] and P. S. Saumia[1,2,§]

[1]*The Institute of Mathematical Sciences, Chennai 600113, India and Homi Bhabha Natitional Institute, Mumbai 400085, India*

[2]*Bogoliubov Laboratory of Theoretical Physics, JINR, 141980 Dubna, Russia*

(Received 27 October 2016; published 11 July 2017)

We study the confinement-deconfinement transition in $SU(2)$ gauge theory in the presence of bosons with vanishing bare mass using lattice Monte Carlo simulations. The nature of this transition depends on the temporal extent (N_τ) of the Euclidean lattice. We find that the transition is a crossover for $N_\tau = 2, 4$ and second order with the three-dimensional Ising universality class for $N_\tau = 8$. Our results show that the second-order transition is accompanied by the realization of the Z_2 symmetry.

DOI: 10.1103/PhysRevD.96.014503

I. INTRODUCTION

Gauge theories such as quantum chromodynamics (QCD), the standard model, etc. at finite temperatures are relevant for describing the phase transitions in the early Universe and in relativistic heavy-ion collisions. The pure gauge parts of these theories undergo the confinement-deconfinement (CD) transition [1,2] at high temperatures. The corresponding pure gauge Euclidean actions are invariant under a class of gauge transformations represented by the center Z_N of the $SU(N)$ group. This Z_N symmetry [3,4] plays an important role in the CD transition. In many ways, the nature of the CD transition is found to be similar to the transition in spin systems with Z_N symmetry. The Z_N symmetry is spontaneously broken in the deconfined phase by a nonzero thermal expectation value of the Polyakov loop. This leads to N degenerate phases in the deconfined state.

In the fundamental representation, the Z_N symmetry is explicitly broken in the presence of the matter fields. The Z_N group can act only on the gauge fields and its action on the matter fields spoils their necessary temporal boundary condition. This explicit breaking affects the nature of the CD transition and the thermodynamic behavior of the phases themselves. It weakens the CD transition and, in the deconfined phase, all but only one of the N phases become metastable. The explicit breaking vanishes when the matter fields are infinitely heavy. So it is expected that the explicit Z_N symmetry breaking is small for large dynamical masses of the matter fields. In the mean-field approximation of QCD, the explicit symmetry breaking turns out to be an effective "uniform" external field acting on the Polyakov loop [5] when the fermion masses are large. The strength of the external field grows as the masses decrease. Nonperturbative studies have found that the CD transition in $SU(2)$ gauge theory with dynamical fermions is a crossover [6–10]. For $SU(3)$ gauge theory, the CD transition becomes a weak first-order transition for large fermion mass [11–15]. These results are consistent with the findings of the mean-field approximation. However, an extrapolation of this effective external field to the chiral limit fails to explain the nature of the CD transition and the Polyakov loop behavior. In this case, the nature of the CD transition turns out to be the same as the chiral transition [16,17]. This suggests that, in the chiral limit, the effective external field is a fluctuating and nonuniform dynamical field instead of a fixed uniform field. The behaviors of the chiral transition and the chiral condensate are, however, well described by a uniform/static field in the chiral limit [18].

It is expected that the explicit breaking of Z_N due to bosonic matter fields also depends on mass. Perturbative calculations show that the explicit symmetry breaking increases with a decrease in mass in the presence of fermionic matter fields [19,20]. A straightforward extension of these one-loop calculations for bosonic fields gives similar results. For the massless case, the explicit symmetry breaking for $N = 2$ is so large that there are no metastable states in the deconfined phase. These calculations, however, are not reliable near the CD transition. Strong coupling studies of lattice non-Abelian gauge theories coupled to the Higgs field with the fixed radial mode have found that the CD transition behaves like a pure gauge CD transition even for some finite nonzero coupling between the gauge and Higgs fields [21]. For heavy Higgs fields, nonperturbative calculations find that the temperature dependence of the Polyakov loop expectation value shows a critical behavior above the CD transition point, i.e. $\langle L\rangle \sim (T - T_c)^{\frac{1}{3}}$ [22,23]. A recent study of the Z_N symmetry [24] showed, within the numerical errors, that the strength of the explicit symmetry breaking vanishes even for a large but finite Higgs mass. These results indicate clear deviations from those of perturbative calculations in the presence of matter fields. It is not clear whether the conventional

*mbiswal@imsc.res.in
†mpdeka@theor.jinr.ru
‡digal@imsc.res.in
§saumia@theor.jinr.ru

expectation that the transition becomes weaker with the mass of matter fields, which is observed in QCD, also holds in the case of $SU(N)$ + Higgs. To address this issue, we study the CD transition in the presence of the Higgs with vanishing bare mass using nonperturbative Monte Carlo simulations. We also compare the nonperturbative and perturbative results away from the CD transition. To simplify our study, we consider $N = 2$ and a vanishing Higgs quartic coupling.

From lattice simulations, it is known that the thermal average of the Polyakov loop [3,20] has a strong cutoff dependence. The Polyakov loop expectation value decreases with the number of temporal sites (N_τ) of the Euclidean lattice. However, the nature of the pure gauge CD transition does not depend on N_τ [25,26]. In the presence of a massless Higgs, this transition is found to be dependent on N_τ. In this study, we find that this transition is a crossover for $N_\tau = 2, 4$ and second order for $N_\tau = 8$. These results suggest that in the continuum limit the CD transition is second order. We also look at the distribution of the Polyakov loop values in the thermal ensemble. The distribution in the case of $N_\tau = 8$ clearly exhibits the Z_2 symmetry, which also explains why the CD transition is second order. This is surprising as one would expect maximal symmetry breaking as is observed in perturbative calculations [19,20] as well as in lattice QCD [15,27]. Coincidentally the realization of the $Z_2(Z_N)$ symmetry occurs only when the system is in the Higgs symmetric phase. This suggests that the strength of the Higgs condensate may be playing the role of the effective external field for the CD transition. We think that this restoration of the $Z_2(Z_N)$ symmetry for larger N_τ is not due to the trivial continuum limit of pure Higgs theories [28] since the interaction between the gauge and Higgs increases with N_τ. We discuss the possible reasons for this realization of Z_2 (or Z_N) symmetry in the Higgs symmetric phase later in Sec. IV.

The paper is organized as follows. In Sec. II we describe the Z_N symmetry in $SU(N)$ + Higgs theory. In Sec. III we describe our simulations and results for $N = 2$. This is followed by conclusions in Sec. IV.

II. THE Z_N SYMMETRY IN THE PRESENCE OF FUNDAMENTAL HIGGS FIELDS

The finite-temperature partition function for a $SU(N)$ gauge field, A_μ, in the path-integral formulation is given by

$$\mathcal{Z} = \int [DA] e^{-S_G}, \tag{1}$$

with the following gauge action:

$$S_G = \int_V d^3x \int_0^\beta d\tau \frac{1}{2}[Tr(F^{\mu\nu}F_{\mu\nu})],$$
$$F_{\mu\nu} = \partial_\mu A_\nu - \partial_\nu A_\mu + g[A_\mu, A_\nu]. \tag{2}$$

The gauge field for a given Euclidean component μ is a $N \times N$ matrix, $A_\mu = T^a A^a_\mu$, where the T^a's are the generators of the $SU(N)$ group. Here β is the inverse of the temperature T. The path integration is over all A_μ's which are periodic along the temporal direction τ, i.e. $A_\mu(\tau) = A_\mu(\tau + \beta)$. This periodicity allows the gauge transformations $U(\tau)$ to be nonperiodic along the temporal direction, up to a factor $z \in Z_N$ as

$$U(\tau = 0) = zU(\tau = \beta). \tag{3}$$

Though the action is invariant under such gauge transformations, the Polyakov loop

$$L(\vec{\mathbf{x}}) = \frac{1}{N}\mathrm{Tr}\left[\mathrm{P}\left\{\exp\left(-ig\int_0^\beta A_0 d\tau\right)\right\}\right], \tag{4}$$

transforms as $L \to zL$. In the deconfined phase L acquires a nonzero expectation value which gives rise to the spontaneous breaking of Z_N symmetry. As a consequence, there are N degenerate states in the deconfined phase characterized by each element of Z_N.

The full Euclidean action in the presence of a bosonic Higgs field Φ is given by

$$S = S_G + \int_V d^3x \int_0^\beta d\tau \left[\frac{1}{2}|D_\mu\Phi|^2 + \frac{m^2}{2}\Phi^\dagger\Phi + \frac{\lambda}{4!}(\Phi^\dagger\Phi)^2\right],$$
$$\text{with} \quad D_\mu\Phi = \partial_\mu\Phi + igA_\mu\Phi. \tag{5}$$

Here m is the mass of the Φ field and λ is the Higgs self-interaction coupling constant. In the partition function

$$\mathcal{Z} = \int [DA][D\Phi] e^{-S}, \tag{6}$$

the path integration of Φ is over all Φ fields which are periodic in τ, i.e. $\Phi(\tau) = \Phi(\tau + \beta)$. Under the action of the above gauge transformations [Eq. (3)], the transformed field $\Phi' = U\Phi$ will not be periodic in τ. So the actions of these gauge transformations have to be restricted to the gauge fields. Consequently, the action will increase under such gauge transformations, i.e. $S(A', \Phi) > S(A, \Phi)$, when the Polyakov loop sector for the configuration A corresponds to the identity of Z_N. It is obvious that the increase in the action will change if the Φ field is varied ($\Phi \to \Phi'$, but $\Phi' \neq U\Phi$) as the gauge fields are gauge transformed. For some Φ configurations, it is possible to find Φ' such that $S(A', \Phi') = S(A, \Phi)$ [24]. If these Φ configurations dominate the partition function, then the Z_N symmetry will be effectively realized. In the following, we describe the simulations of the CD transition for $N = 2$ and $m = 0 = \lambda$ using the above partition function.

III. SIMULATIONS OF THE CONFINEMENT-DECONFINEMENT TRANSITION

In the Monte Carlo simulations, the Euclidean space is discretized into $N_\tau \times N_s^3$ discrete points. $N_\tau = 1/(aT)$ and $N_s = (L/a)$ are the number of lattice points along the temporal and spatial directions, respectively. a is the lattice spacing and L is the spatial extent of the Euclidean space. Each point n on the lattice is represented by a set of four integers, i.e. $n = (n_1, n_2, n_3, n_4)$. The Higgs field Φ_n lives on the lattice site n. The gauge link $U_\mu = \exp(-iagA_\mu)$, on the other hand, lives on the link connecting the point n to its nearest neighbor along the positive μ direction. The action with these discretized field variables with appropriate scaling in terms of a for $m = 0 = \lambda$ is given by [29],

$$S = \beta \sum_p \mathrm{Tr}\left(1 - \frac{U_p + U_p^\dagger}{2}\right) - \frac{1}{8}\sum_{\mu,n} \mathrm{Re}[(\Phi^\dagger_{n+\mu} U_{n,\mu} \Phi_n)] + \frac{1}{2}\sum_n (\Phi_n^\dagger \Phi_n). \quad (7)$$

In Eq. (7), the first term represents the pure gauge action. U_p is the product of the gauge links going counterclockwise on the pth elementary square/plaquette on the lattice. The Polyakov loop at any spatial point n is given by the path order product of links on the shortest temporal loop going through n. The gauge transformation [Eq. (3)] of the gauge fields is equivalent to the multiplication of all the temporal links on a fixed τ slice by $z \in Z_N$. The second term represents the interaction of the gauge and Higgs fields. This term is not invariant under the gauge transformations [Eq. (3)] of the gauge fields while the Φ field configuration is kept fixed. As mentioned above, the Φ fields cannot be transformed under nonperiodic gauge transformations.

In the Monte Carlo simulations, a sequence of statistically independent configurations of $(\Phi_n, U_{\mu,n})$ are generated. This is achieved by repeatedly updating an arbitrary initial configuration using numerical methods which follow the Boltzmann probability factor e^{-S} and the principle of detailed balance among the configurations in the sequence. To update the gauge fields, we first use the standard heat bath algorithm [30,31], and then update the Higgs fields using the pseudo–heat bath algorithm [32]. We then again update the gauge fields using four over-relaxation steps [33] after which the Higgs fields are updated again using the pseudo–heat bath algorithm. To reduce autocorrelation between successive configurations along the sequence (Monte Carlo history) we carry out ten cycles of this updating procedure between subsequent measurements. For our simulations, we use the publicly available MILC code [34] and modify it to accommodate the Higgs fields.

The CD transition is studied for three values of $N_\tau = 2, 4$ and 8. For $N_\tau = 2$, we consider three spatial volumes, $N_s = 8$, 10, 12. For $N_\tau = 4$, we consider $N_s = 16$, 20 and 24. For $N_\tau = 8$, we consider $N_s = 32$, 40 and 48. For each volume, we analyze 100 000 configurations. However, we have lower statistics for β values far away from β_c, particularly for the two biggest volumes $40^3 \times 8$ and $48^3 \times 8$. The Polyakov loop, susceptibility and Binder cumulant are computed for various values of β to locate the transition point. We carry out the error analysis using the jackknife method with a bin size of 10 000 configurations. We also compute the volume average of $\Phi^\dagger\Phi$ and the interaction term. It is important to note that even though the Φ field is massless at the tree level, the fluctuations are finite. This is because the interaction with the gauge fields generates a nonzero finite mass for the Φ field. In the following section, we describe our simulation results.

A. The CD transition for $N_\tau = 2$ and 4

The Polyakov loop $\langle|L|\rangle$ vs β for $N_\tau = 2$ and $N_\tau = 4$ are shown in Figs. 1(a) and 1(b), respectively. $\langle|L|\rangle$ grows with β with a sharp increase around the transition. The one-loop

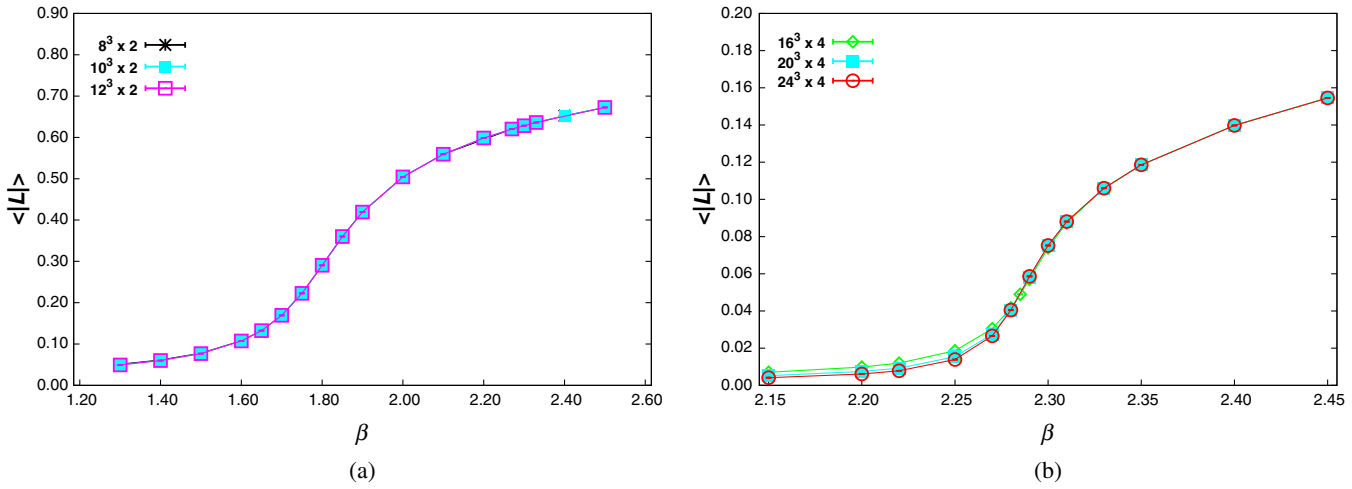

(a) (b)

FIG. 1. The Polyakov loop average vs β for (a) $N_\tau = 2$, and (b) $N_\tau = 4$.

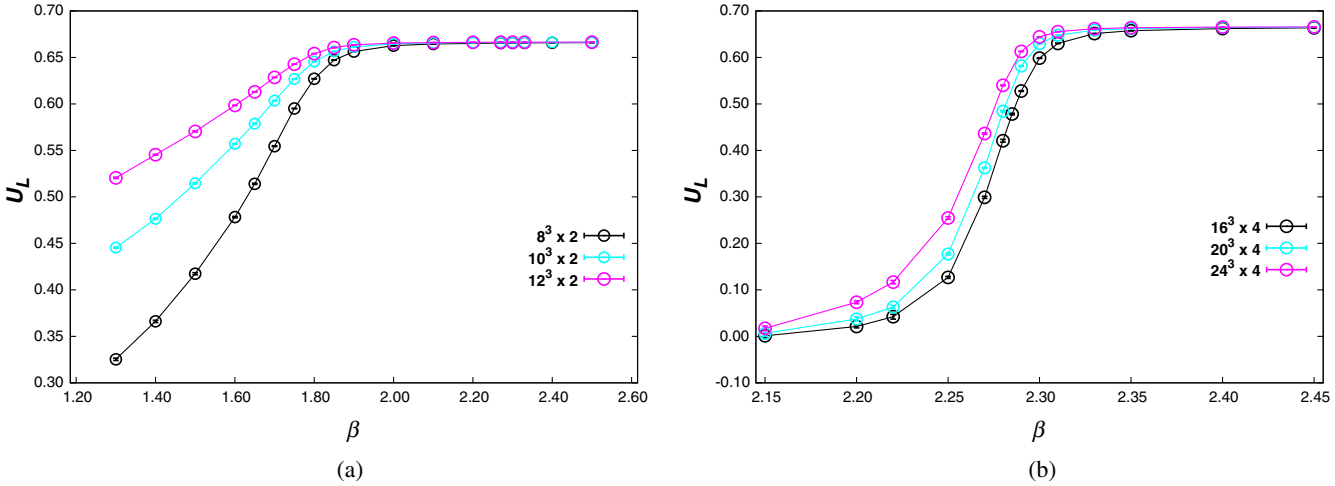

FIG. 2. U_L vs β for different volumes for (a) $N_\tau = 2$, and (b) $N_\tau = 4$.

β-function temperature dependence of $\langle|L|\rangle$ is found to be consistent with the power law, $\langle|L|\rangle \sim (T - T_c)^{1/3}$ [23]. However $\langle|L|\rangle$ does not show any volume dependence. The peak height of the Polyakov loop susceptibility does not vary with volume.

The Binder cumulant [35]

$$U_L = 1 - \frac{\langle L^4 \rangle}{3\langle L^2 \rangle^2}, \tag{8}$$

for different β are shown in Figs. 2(a) and 2(b) for $N_\tau = 2$ and $N_\tau = 4$, respectively. In both cases the variation in U_L decreases for larger volumes. For $N_\tau = 2$, U_L is almost flat against β. This behavior of the Binder cumulant is exactly the opposite of what is expected in a second-order phase transition. The only explanation for these results is that the correlation length is finite and does not grow with volume. The sharp variation of the Polyakov loop around $\beta_c \sim 1.8(N_\tau = 2)$ and $\beta_c \sim 2.29(N_\tau = 4)$ only suggests a crossover for the CD transition.

B. The CD transition for $N_\tau = 8$

The behavior of the Polyakov loop for $N_\tau = 8$ is completely different from that of $N_\tau = 2$ and 4. The Polyakov loop $\langle|L|\rangle$ around the transition point β_c behaves almost like the magnetization in the Ising model. The results for $\langle|L|\rangle$ vs β for different volumes are shown in Fig. 3(a). In this case, $\langle|L|\rangle$ clearly shows a volume dependence. The volume dependence of the susceptibility χ^c of the Polyakov loop around the transition point is shown in Fig. 4(a). In Figs. 3(b) and 4(b), we show the magnetization and susceptibility vs $(L^{1/\nu}(\beta - \beta_c)/\beta_c)$, respectively. We see that both quantities collapse to single curves.

We find the value of the exponent, γ/ν, by studying the finite-size scaling of the location of the maxima of the χ^c's similar to Ref. [36]. However instead of using the reweighting method to determine $\chi^c_{\max}$, we use the cubic spline interpolation method to generate a few hundred points close to $\beta_{\chi_{\max}}$ for every jackknife sample since we have a

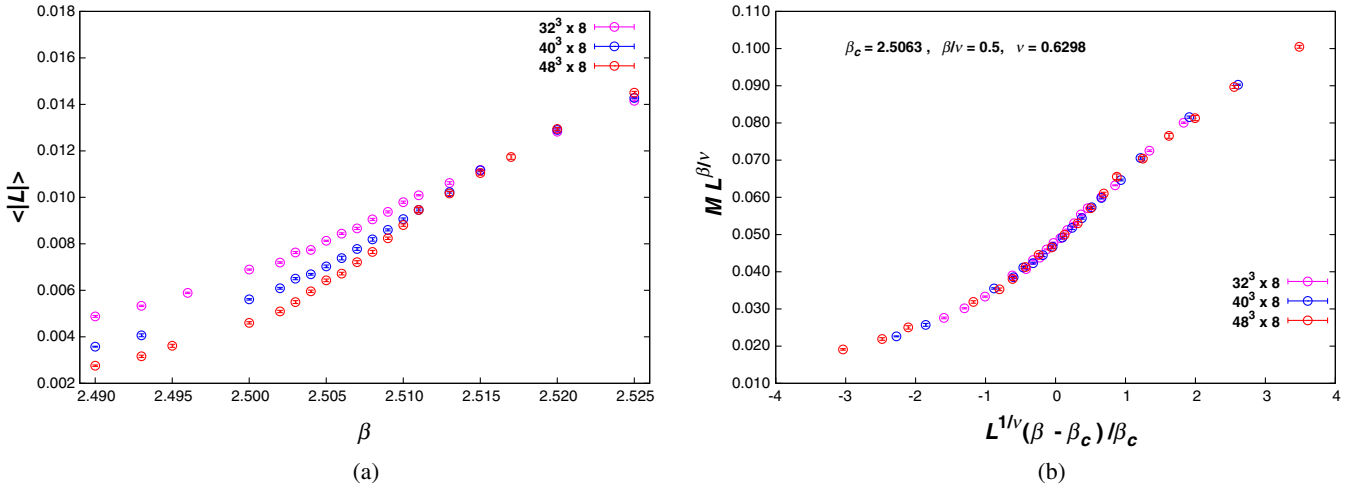

FIG. 3. $N_\tau = 8$. (a) The Polyakov loop vs β for different volumes, and (b) the scaled Polyakov loop vs β for different volumes.

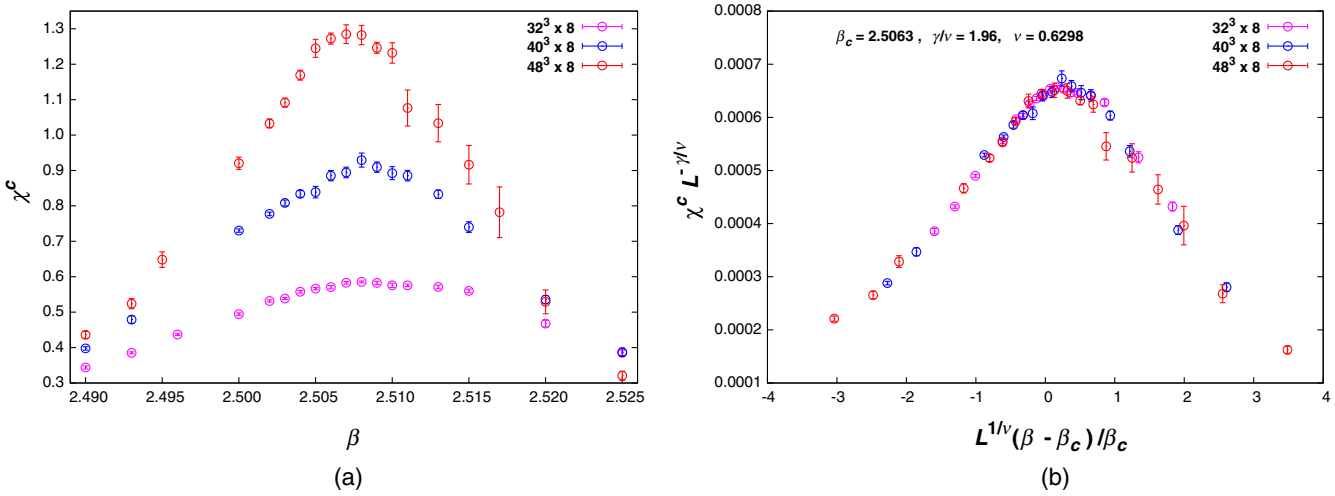

FIG. 4. $N_\tau = 8$. (a) Susceptibility vs β for different volumes, and (b) the scaled susceptibility vs β for different volumes.

reasonable amount of data near the peak for each volume. The scaling behavior of $\chi^c_{\max}$ as a function of spatial volume, L, is shown in Fig. 6(a). We obtain $\gamma/\nu = 1.97(4)$.

The Binder cumulant for $N_\tau = 8$ is shown in Fig. 5(a). While the $U_L(\beta)$ for different volumes do not intersect for $N_\tau = 2$ and 4, they do for $N_\tau = 8$ in a narrow region around the transition point. To determine β_c and the corresponding value of the Binder cumulant, we use the following finite-size behavior of U_L in the vicinity of the critical point:

$$U_L \approx a_0 + a_1(\beta - \beta_c)/\beta_c L^{1/\nu} + a_2 L^{-\omega} + \cdots. \quad (9)$$

By following the same procedure as in Ref. [37], we can write

$$\beta_c^{\text{eff}} = \beta_c(1 - \alpha\epsilon), \quad \text{where } \epsilon = L^{-1/\nu-\omega}\frac{1 - b^{-\omega}}{b^{1/\nu} - 1},$$
$$b = \frac{L'}{L}, \qquad b > 1. \quad (10)$$

The crossing point of the straight lines of two different spatial volumes provides β_c^{eff}. By using the three-dimensional (3D) Ising values of $\nu = 0.6298$ and $\omega = 0.825$, we obtain β_c in the limit $\epsilon \to 0$ as $\beta_c = 2.5063(4)$. Figure 5(b) shows that U_L vs $(L^{1/\nu}(\beta - \beta_c)/\beta_c)$ for different volumes collapse to a single curve. To obtain the infinite-volume Binder cumulant, U_c, we use the following relation:

$$U_c^{\text{eff}} = U_c(1 + \alpha'\epsilon'), \quad \text{where } \epsilon' = L^{-\omega}\frac{1 - b^{-\omega-1/\nu}}{1 - b^{-1/\nu}}. \quad (11)$$

In Fig. 6(b), we show U_c^{eff} vs ϵ'. In the limit $\epsilon' \to 0$, we obtain $U_c = 0.468(4)$. To determine the exponent β/ν, we find the magnetization at β_c for each volume using cubic spline interpolation. Using $\langle|L|\rangle|_{\beta_c} \sim L^{\beta/\nu}$, we get $\beta/\nu = 0.53(3)$.

The above values of β/ν, γ/ν and $U_L(\beta_c)$ from our computations are close to the 3D Ising values. These results

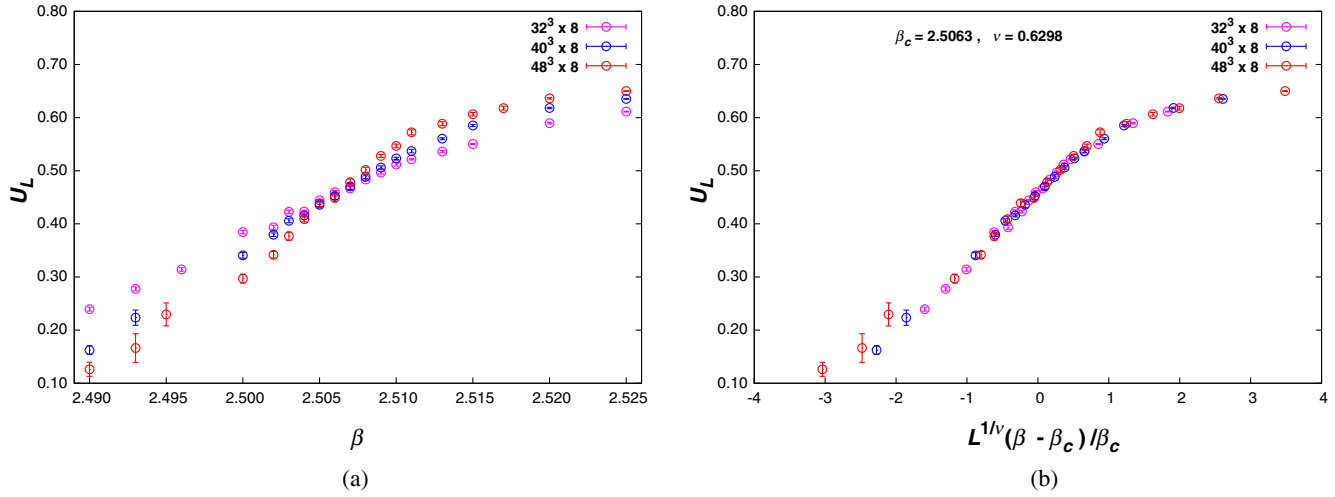

FIG. 5. $N_\tau = 8$. (a) The Binder cumulant U_L vs β for different volumes, and (b) the scaled U_L vs β for different volumes.

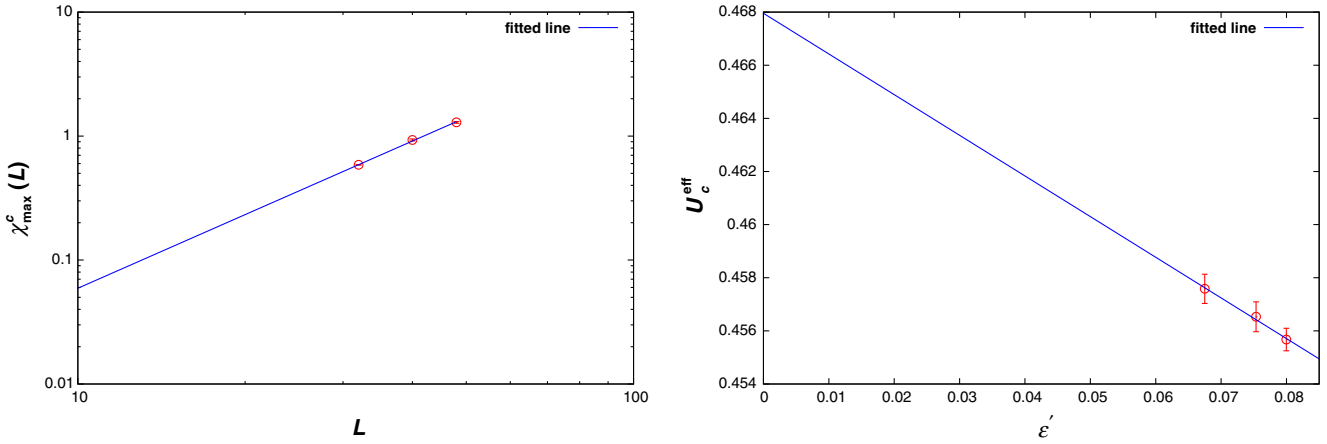

FIG. 6. $N_\tau = 8$. (a) The values of $\chi^c_{\max}$ as a function of L for $L = 32$, 40 and 48. The slope of the fitted line provides the value of γ/ν. (b) The values of $U_c^{\rm eff}$ obtained from the crossing points of the Binder cumulant between two different volumes as a function of ϵ'. The intercept provides the value of U_c.

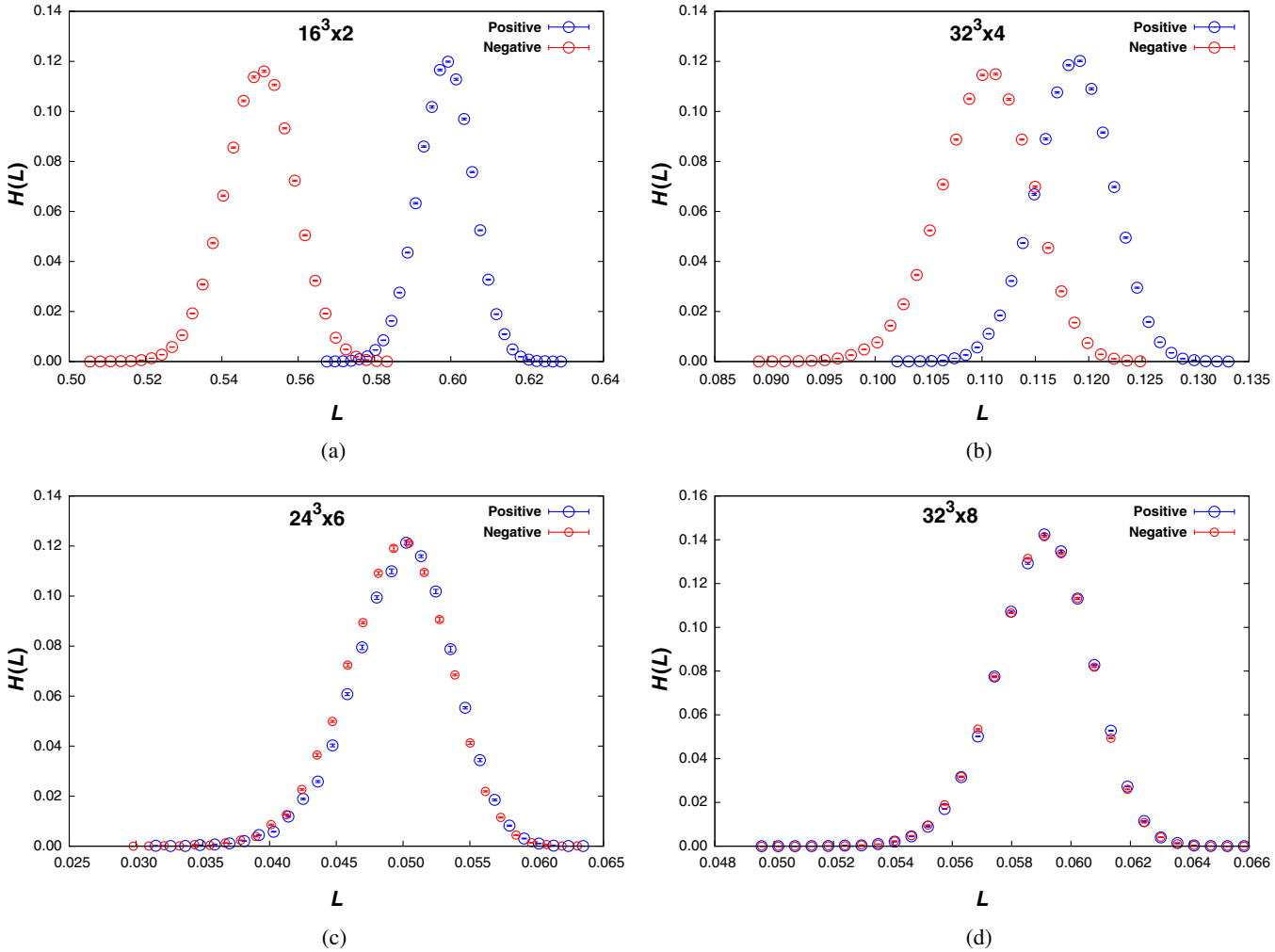

FIG. 7. $H(L)$ vs $|L|$. $H(L)$ is normalized to 2. (a) $16^3 \times 2$ lattice with $\beta = 2.20$, (b) $32^3 \times 4$ lattice with $\beta = 2.35$, (c) $24^3 \times 6$ lattice with $\beta = 2.50$, and (d) $32^3 \times 8$ lattice with $\beta = 3.20$.

seem to show that the CD transition transition for $N_\tau = 8$ is a second-order phase transition.

C. The Z_2 symmetry of the Polyakov loop

The different N_τ studies clearly show that the nature of the CD transition depends on N_τ. The change in the nature of the CD transition from $N_\tau = 8$ to $N_\tau = 2, 4$ is similar to that of the Ising transition when the external field is increased. So it is possible that the explicit breaking of the Z_2 symmetry decreases with an increase in N_τ. To check this, we compute the histogram of the Polyakov loop near the transition point for $N_\tau = 2$, 4 and 8. For $N_\tau = 2$ and 4, no Z_2 symmetry is observed in the distribution of the Polyakov loop. On the deconfinement side and close to the transition point, the histograms always show one peak located on the positive real axis. Away from the transition point and inside the deconfinement phase, locally stable states are observed for which the Polyakov loop is negative. In Fig. 7(a) the histogram of the Polyakov loop $H(L)$ vs $|L|$ for $\beta = 2.2$ is shown for $N_\tau = 2$. $H(L)$ is normalized to 2. There is no Z_2 symmetry between either the locations or the widths of the peaks. So the behavior of the Polyakov loop such as the thermal average, fluctuations, correlation length, etc. are found to be different for these two states. In contrast, the Polyakov loop exhibits Z_2 symmetry for $N_\tau = 8$. Near the transition point, two peaks symmetrically located around $L = 0$ on the real x axis are observed. In Fig. 7(d), $H(L)$ vs $|L|$ is shown for $\beta = 3.20$. Though 10^6 measurements are used to compute all the data points in Fig. 7(d), each individual point in the figure is the average over $(H(L) * 10^6)$ configurations for which the Polyakov loop values belong to a small bin centered at L. For example, the peaks of the histogram result from about $\sim 1.5 \times 10^4$ configurations. It is interesting to see that $H(L)$ for $+L$ and $-L$ agree even with such small statistics. All physical observables which depend on the temporal gauge field such as the gauge action and interaction term have the same average when computed for the two Z_2 sector. These

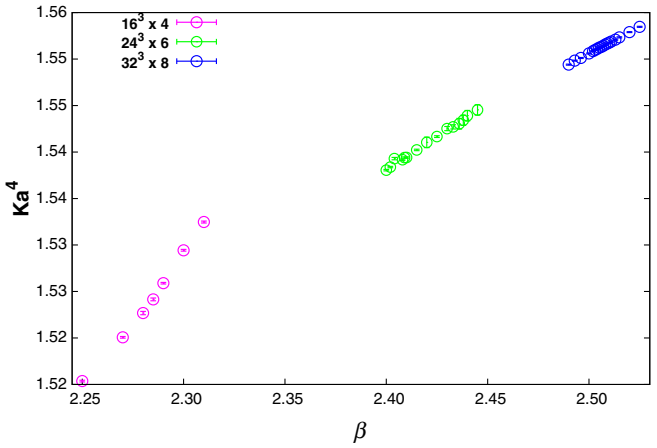

FIG. 8. Ka^4 near β_c for different N_τ.

results suggest the effective realization of the Z_2 symmetry for $N_\tau = 8$. We find that the ensemble average of the interaction term, $Ka^4 = \frac{1}{8}\sum_{\mu,n} \mathrm{Re}(\Phi^\dagger_{n+\mu} U_{n,\mu} \Phi_n)$ in Eq. (7), increases with N_τ. In Fig. 8, we plot the average of Ka^4 per site near β_c for $N_\tau = 4$, 6 and 8. From the one-loop beta function [23], the lattice spacing near the transition point for $N_\tau = 8$ is smaller compared to those of $N_\tau = 4$ and 6. This implies that the interaction K in physical units is larger for $N_\tau = 8$. Our results suggest that K in the continuum limit will remain finite. The mass in lattice units, extracted from correlators of gauge-invariant operators constructed from the Higgs fields and link variables [38,39], decreases from $N_\tau = 4$ to $N_\tau = 8$. This seems to support that the restoration of Z_2 is due to the enhancement of the Higgs phase space due to an increase in N_τ.

IV. DISCUSSIONS AND CONCLUSIONS

In this work, we studied the CD transition and Z_2 symmetry in $SU(2)$ + Higgs theory for a vanishing bare mass and quartic coupling of the Higgs field. We found that the cutoff effects are large. For $N_\tau = 2$ and 4, the CD transition turns out to be a crossover. The temperature dependence of the Polyakov loop average seems to show a critical behavior above the crossover point. However, no volume dependence is observed in any observable related to the Polyakov loop. For $N_\tau = 8$, the temperature dependence, susceptibility and the Binder cumulant of the Polyakov loop show singular behavior suggesting a second-order CD transition. Our results for the critical exponents are found to be consistent with the 3D Ising universality class.

The singular behavior of the Polyakov loop for $N_\tau = 8$ is accompanied by the effective realization of the Z_2 symmetry. Z_2 symmetric peaks were observed in the histogram of the Polyakov loop in the deconfined phase near the transition point. Thermal averages such as the fluctuations of the Polyakov loop, the interaction term between the gauge and the Higgs field, the gauge action, etc. were all found to be same for the two deconfined states related by Z_2 symmetry. Note that the interaction between the Higgs and gauge fields are nonzero which implies that the realization of the Z_2 symmetry is not due to the vanishing or small interaction. We observed that the interaction in a given physical volume increases with N_τ. From $N_\tau = 4$ to 6, the interaction increases by a factor of ~ 5 and, from $N_\tau = 6$ to 8, it increases by a factor of ~ 3. In our simulations, we found that fluctuations of the Higgs field play an important role. A Z_2 flip of the gauge fields is always accompanied by a "realignment" ($\Phi \to \Phi'$) of the Higgs configuration. As soon as the Higgs fluctuations are frozen/fixed, the explicit breaking of Z_2 reappears. The reason why the Z_2 realization happens for $N_\tau = 8$ and not for $N_\tau = 2$ and 4 is the increase in the phase space of the Φ field with N_τ. With the increase in the phase space, it is more likely that for a given Φ there exists a Φ' which can

compensate for the increase in the action due to the Z_2 rotation of the gauge fields. We find that the likelihood of finding such a Φ' increases with N_τ. It is important to note that the Z_2 symmetry in our simulations only implies that a Φ' exists for every statistically significant Φ. It is obvious that there will be Φ configurations for which there will not be any Φ' even in the limit $N_\tau \to \infty$. This is expected to happen when the Higgs field acquires a condensate. In this sense, the restoration/realization of the Z_2 symmetry is not exact, and the explicit symmetry breaking is not zero but statistically insignificant.

Our results may have important implications for the study of Z_N symmetry in the presence of matter fields. Conventionally, it is expected that in the massless limit there will be maximal breaking of the Z_2 symmetry and the CD transition will be a crossover. One-loop perturbative calculations [19,20] for fermions suggest that the explicit breaking for the massless case will be so large that there will be no metastable states in the entire deconfinement phase. A straightforward extension for bosonic fields gives similar results. However, our nonperturbative results suggest that the explicit breaking is so minimal that metastable states tend to become degenerate with the stable state in the continuum. It would be interesting to see if a similar realization of the Z_N symmetry happens for different N and also in the presence of fermion fields. We plan to study these issues in our future work.

ACKNOWLEDGMENTS

All of our numerical computations have been performed at the Annapurna super cluster based at the Institute of Mathematical Sciences, India and HybriLIT super cluster based at Joint Institute for Nuclear Research, Dubna, Russia. We have used the MILC Collaboration's public lattice gauge theory code (version 6) [34] as our base code.

[1] J. Kuti, J. Polonyi, and K. Szlachanyi, Phys. Lett. **98B**, 199 (1981).
[2] L. D. McLerran and B. Svetitsky, Phys. Lett. **98B**, 195 (1981).
[3] B. Svetitsky, Phys. Rep. **132**, 1 (1986).
[4] B. Svetitsky and L. G. Yaffe, Nucl. Phys. **B210**, 423 (1982).
[5] F. Green and F. Karsch, Nucl. Phys. **B238**, 297 (1984).
[6] A. Nakamura, Phys. Lett. **149B**, 391 (1984).
[7] U. M. Heller and F. Karsch, Nucl. Phys. **B258**, 29 (1985).
[8] U. M. Heller, Phys. Lett. **163B**, 203 (1985).
[9] J. B. Kogut, J. Polonyi, H. W. Wyld, and D. K. Sinclair, Phys. Rev. D **31**, 3307 (1985).
[10] J. B. Kogut, J. Polonyi, H. W. Wyld, and D. K. Sinclair, Nucl. Phys. **B265**, 293 (1986).
[11] J. Polonyi, H. W. Wyld, J. B. Kogut, J. Shigemitsu, and D. K. Sinclair, Phys. Rev. Lett. **53**, 644 (1984).
[12] P. Hasenfratz, F. Karsch, and I. O. Stamatescu, Phys. Lett. **133B**, 221 (1983).
[13] R. V. Gavai and F. Karsch, Nucl. Phys. **B261**, 273 (1985).
[14] M. Fukugita and A. Ukawa, Phys. Rev. Lett. **57**, 503 (1986).
[15] F. Karsch, E. Laermann, and C. Schmidt, Phys. Lett. B **520**, 41 (2001).
[16] S. Digal, E. Laermann, and H. Satz, Nucl. Phys. **A702**, 159 (2002).
[17] K. Fukushima, Phys. Lett. B **553**, 38 (2003).
[18] R. D. Pisarski and F. Wilczek, Phys. Rev. D **29**, 338 (1984).
[19] D. J. Gross, R. D. Pisarski, and L. G. Yaffe, Rev. Mod. Phys. **53**, 43 (1981).
[20] N. Weiss, Phys. Rev. D **25**, 2667 (1982).
[21] E. H. Fradkin and S. H. Shenker, Phys. Rev. D **19**, 3682 (1979).
[22] P. H. Damgaard and U. M. Heller, Nucl. Phys. **B294**, 253 (1987).
[23] P. H. Damgaard and U. M. Heller, Phys. Lett. B **171**, 442 (1986).
[24] M. Biswal, S. Digal, and P. S. Saumia, Nucl. Phys. **B910**, 30 (2016).
[25] S. Datta and R. V. Gavai, Phys. Rev. D **60**, 034505 (1999).
[26] J. B. Kogut, M. Stone, H. W. Wyld, W. R. Gibbs, J. Shigemitsu, S. H. Shenker, and D. K. Sinclair, Phys. Rev. Lett. **50**, 393 (1983).
[27] S. Digal, E. Laermann, and H. Satz, Eur. Phys. J. C **18**, 583 (2001).
[28] D. J. E. Callaway, Phys. Rep. **167**, 241 (1988).
[29] K. Kajantie, M. Laine, K. Rummukainen, and M. E. Shaposhnikov, Nucl. Phys. **B466**, 189 (1996).
[30] M. Creutz, Phys. Rev. D **21**, 2308 (1980).
[31] A. D. Kennedy and B. J. Pendleton, Phys. Lett. **156B**, 393 (1985).
[32] B. Bunk, Nucl. Phys. B, Proc. Suppl. **42**, 566 (1995).
[33] C. Whitmer, Phys. Rev. D **29**, 306 (1984).
[34] http://www.physics.utah.edu/~detar/milc/.
[35] K. Binder, Z. Phys. B **43**, 119 (1981).
[36] K. Kanaya and S. Kaya, Phys. Rev. D **51**, 2404 (1995).
[37] J. Fingberg, U. M. Heller, and F. Karsch, Nucl. Phys. **B392**, 493 (1993).
[38] B. Bunk, E. M. Ilgenfritz, J. Kripfganz, and A. Schiller, Nucl. Phys. **B403**, 453 (1993).
[39] B. Bunk, E. M. Ilgenfritz, J. Kripfganz, and A. Schiller, Phys. Lett. B **284**, 371 (1992).